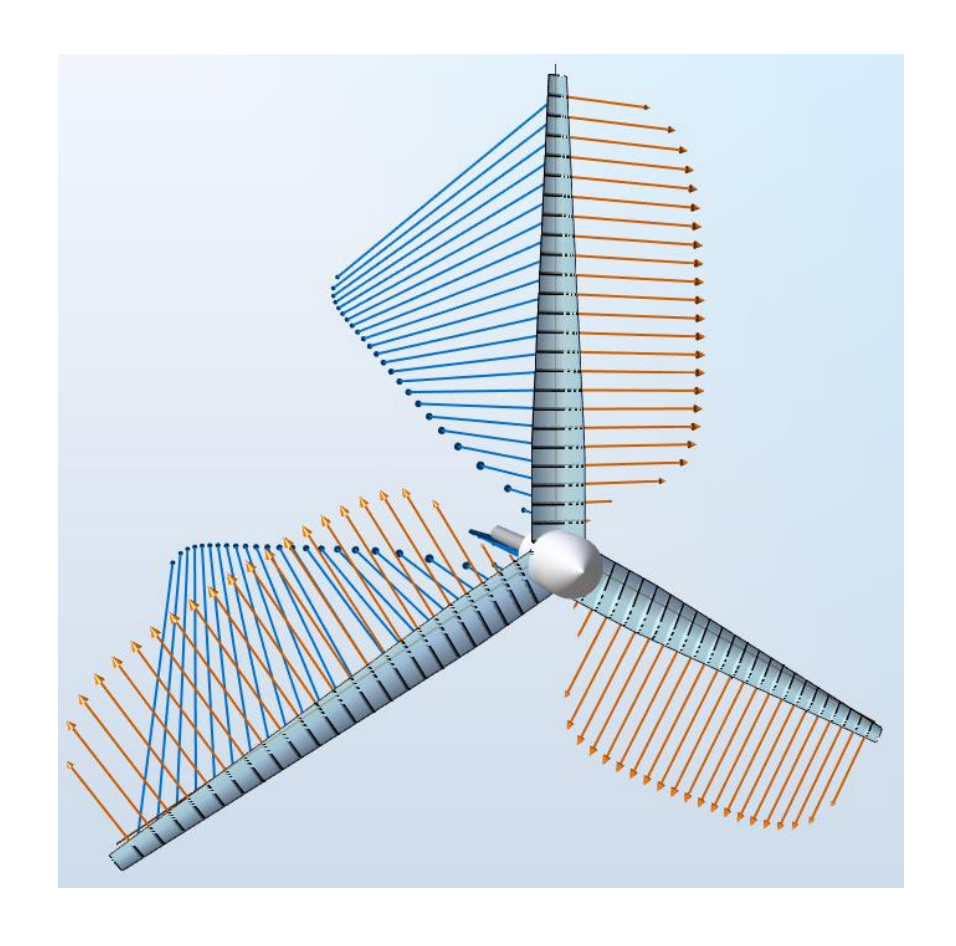


Blade Optimisation

ME40123 Design Optimisation



Harry Mills (12196)

Word count: 2980

12-Jan-2024

Contents

1 Int	I Introduction	
1.1	Regulations	1
1.2	Design space & Assumptions	2
2 Op	otimisation	2
2.1	Chord Length	4
2.2	Twist Angle	6
2.3	Airfoil Section	8
3 Results		12
3.1	Optimisation discussion	14
4 Re	flection	15
4.1	Improved Parameterisation	15
4.2	Objective Function	16
4.3	Manufacturing Considerations	16
References		

Abbreviations

HAWT Horizontal axis wind turbine

SWT Small wind turbine

AEP Annual energy production

 C_p Coefficient of Power

TSR Tip speed ratio (λ)

1 Introduction

Wind turbines harness the kinetic energy of wind to generate electricity using aerodynamic forces on the rotor blades. The most common type of wind turbine (and the focus of this study) are horizontal axis wind turbines where the shaft of the rotor points in the direction of the wind, as opposed to vertical axis wind turbines.

Commercial power generating wind turbines average a nominal capacity of 3.2 MW, and 130m diameter[1]. However, there is renewed interest in small wind turbines (SWT) for offgrid, decentralised power generation. SWTs have not received the same level of aerodynamic refinement as large turbines, so current SWT have lower efficiency and therefore a higher cost of energy.

1.1 Regulations

In the UK, general permitted development under the town and country planning act (2015)[2][3] sets the dimensions of small wind turbines that can be installed on residential property without planning permission. For this study, the key details are:

- 15m maximum height when attached to a building (11m standalone),
- Minimum ground to blade distance is more than 5m,
- Swept area of any blade is **3.8m²** maximum.

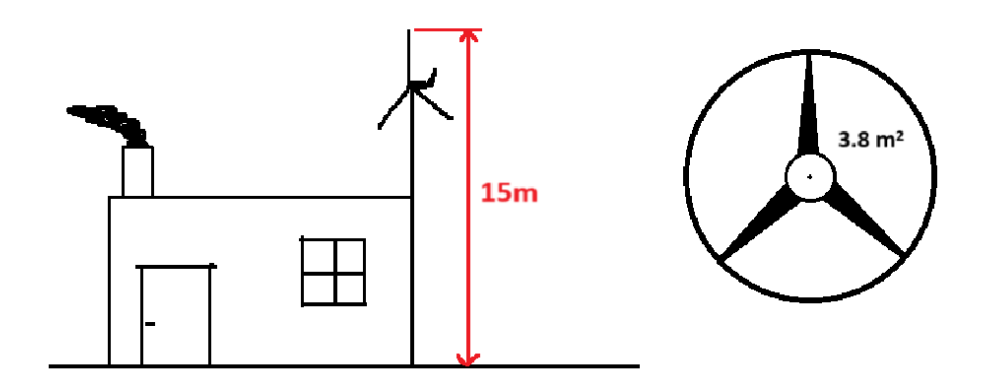


Figure 1 Visual summary of class H regulations for residential wind turbines

The maximum swept area of a blade can be used to calculate the maximum blade length:

$$\pi r^2 = 3.8m^2$$

$$r = \sqrt{\frac{3.8}{\pi}} = 1.0998 \approx 1.1m$$

The regulations are ambiguous whether 'swept blade area' includes the nacelle. For simplicity this study will disregard nacelle size and diameter, focusing purely on blade shape optimisation for a 1.1m blade.

1.2 Design space & Assumptions

After deciding on a blade length of 1.1m, further assumptions were made to focus the study and simplify the problem due to time constraints:

- Stiff blade: Structural considerations (bending/fatigue) are not considered in this study.
- Assembly: The nacelle and how blades are attached are not considered.
- Steady state: Turbulent wind conditions or transient wind are not considered.

The key design variables of the blade optimisation are:

- Chord length
- Twist angle
- Airfoil section

These will be varied programmatically to perform an optimisation of a 1.1m length small wind turbine blade. The blade will be separated into 25 'stations' which can have individually varied chord, twist, and airfoil section.

2 Optimisation

For the initial optimisation the coefficient of power (C_p) was used. This represents how much energy is being extracted from the wind flow. The limit for a wind turbine is 59% (Betz limit[4]), however real wind turbines have C_p values between 40%-53%[5].

The maximum C_p of a blade was found by running several simulations on the blade at a range of tip speed ratios (TSR). TSR refers to the ratio of the linear speed of the blade tip to the incoming free stream velocity. The most efficient TSR ratio depends on the number of blades. 3-blade turbines have TSRs between 5-7, whereas a 10-blade turbine might operate most efficiently at λ =3 [6]. Initially, in this study a 3 bladed design was used and simulated over TSRs between 3-9 to generate a C_p vs TSR curve, the maximum of this curve being returned as the objective function.

Figure 2 shows the framework of the optimisation. The optimiser calls the objective function, CpMax.m, which in turn calls sub-functions to calculate the distribution of chord, twist, and airfoil, before running the simulation in Ashes to calculate the C_p at each TSR.

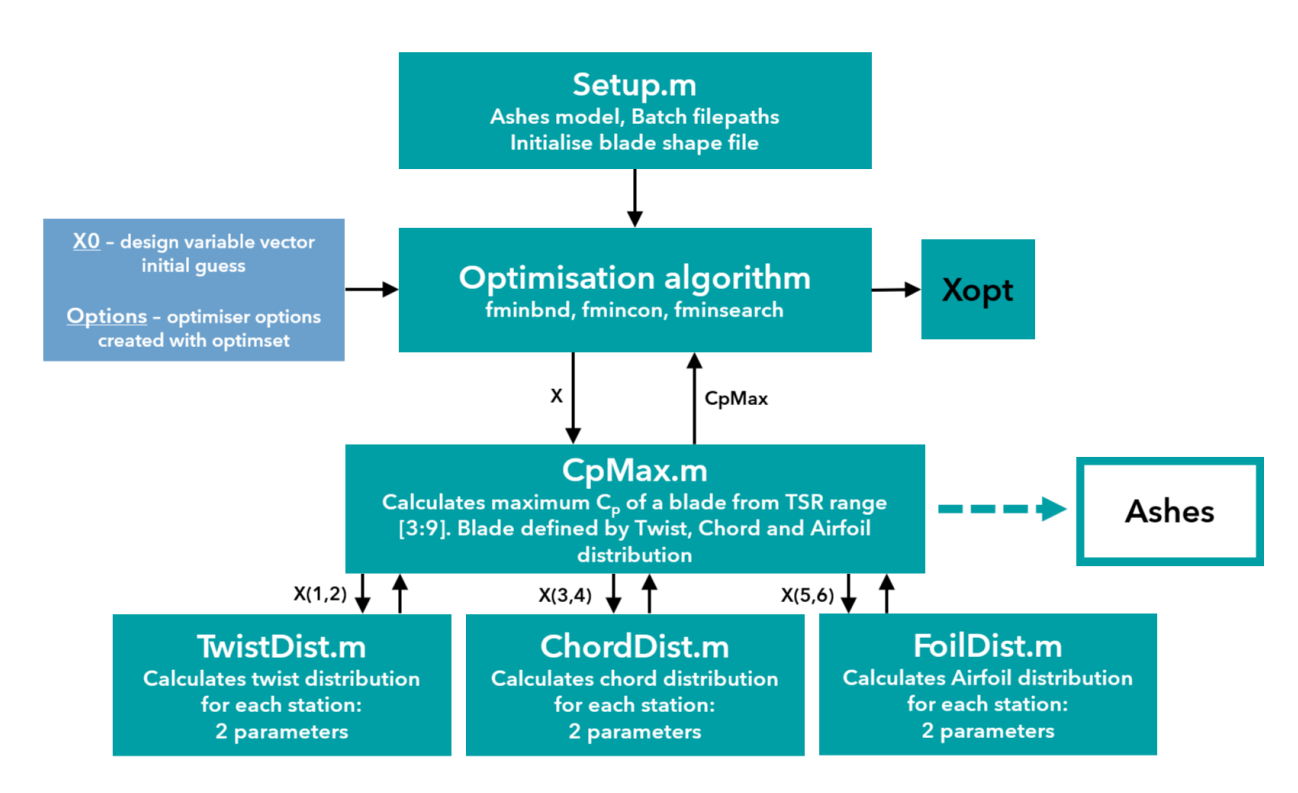


Figure 2 Blade optimisation framework

For this study, 25 equally spaced points along the wind turbine blade were defined as aerodynamical stations where each parameter could be varied, with the blade cross-section smoothly blending between each station.

As a baseline, a non-twisted, constant chord and airfoil blade was simulated across the range of TSRs. Figure 3 shows this blade and the C_p vs TSR characteristics. The maximum C_p =**38.31%** for this blade (λ =5.5)

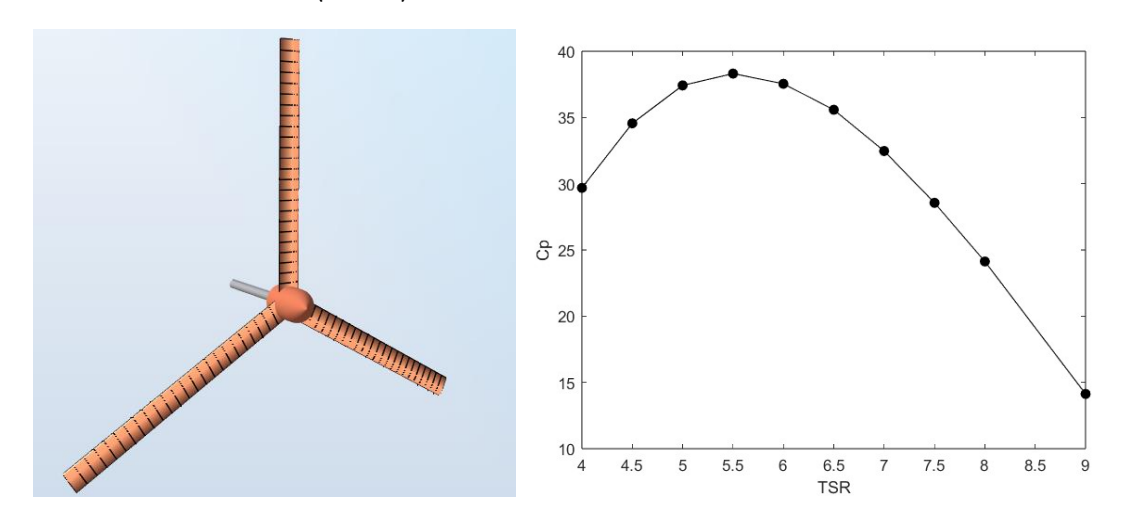


Figure 3 Left: Ashes model of the constant cross-section, untwisted blade. Right: Cp vs TSR graph to show that the maximum Cp of the blade (38.3%) occurs at TSR = 5.5

2.1 Chord Length

Stylianidis (2010)[7], recommends linearisation of the chord distribution as one of the most common simplifications to reduce manufacturing cost and complexity of blades.

Figure 4 shows how the chord distribution may be parameterised for <u>aerodynamic</u> optimisation. The root chord length (d')(0-20% of radius), and the tip chord length (d_3) are the 2 variables. Chord length is then linear from 20-100% of the radius. Varying these then changes the chord length at every station, rather than inefficiently using 20+ design variables to individually vary chord length at each station, which would be much more computationally expensive and difficult to manufacture. This simplification therefore increases the optimisation algorithm speed, while also incorporating manufacturing considerations by constraining the chord to a linear distribution.

Structural considerations are not part of this study, but it is important to note that the root section of the blade (up to ~20% of radius) does not contribute significantly to generating aerodynamic forces, but it is critical for supporting the load (Figure 5)[8]. For the purposes of this study, chord length is constrained to be constant from 0-20% of the blade length.

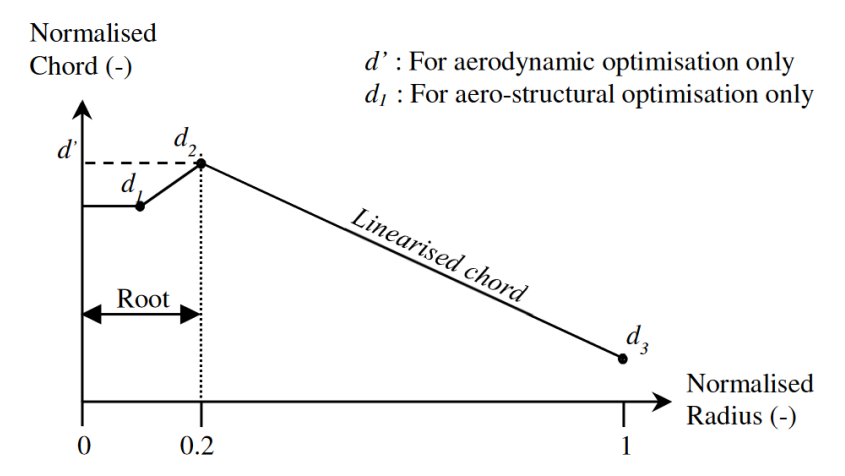


Figure 4 Simplified chord distribution parameterisation from Stylianidis (2010). d' is the root chord length, d3 is the tip chord length.[7]

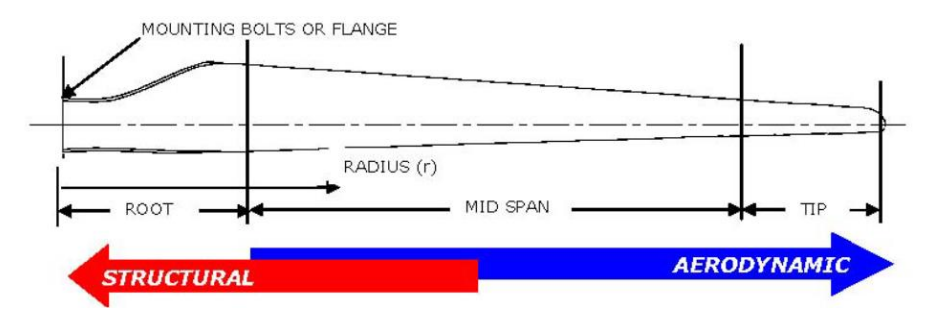


Figure 5 Chord distribution of a wind turbine blade optimised for aerodynamic and structural considerations.[8]

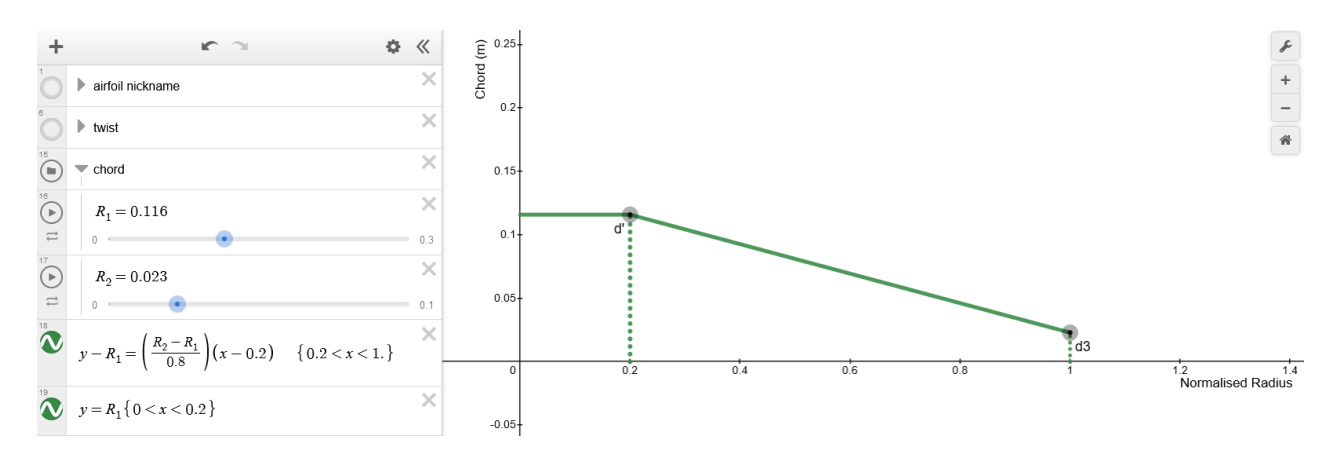


Figure 6 Graph with equations embodying the parameterisation described in Stylianidis (2010)[7] to vary chord length along the blade for aerodynamic optimisation.

ChordDist.m is the function called by the objective function to generate the new chord distribution based on the current design variable vector (Figure 2). This uses the equations shown in Figure 6 to generate the chords for each aerodynamical station.

Stylianidis (2010)[7], argues that even though single parameter optimisations will not be the most optimal, they are still valuable because the result will be near optimal and is much less computationally demanding. For example, optimising the chord distribution without changing twist and airfoil is a useful starting point not just to sanity check any results but also will provide a near optimal chord distribution.

Figure 7 shows the convergence plot for the 2-dimensional optimisation of the chord length.

As objective function gradient data is not available, a gradient-free approach was required. The Nelder-Mead algorithm was used, which may get stuck in local minima, but will find a minimum efficiently. Initially, the design space was assumed to be convex, but multiple starting guess could be used to evaluate how true this is. Alternatively, a global search (e.g.: genetic algorithm) could be used be used, which would guarantee the global minimum is found, but would take more function evaluations to get very close to the optimum location.

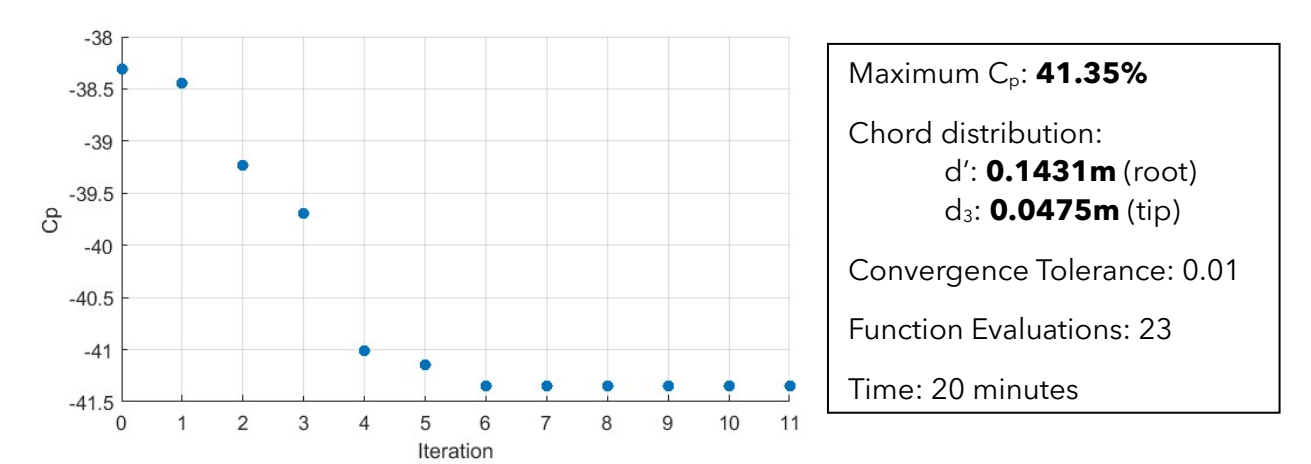


Figure 7 Convergence plot for chord distribution optimisation

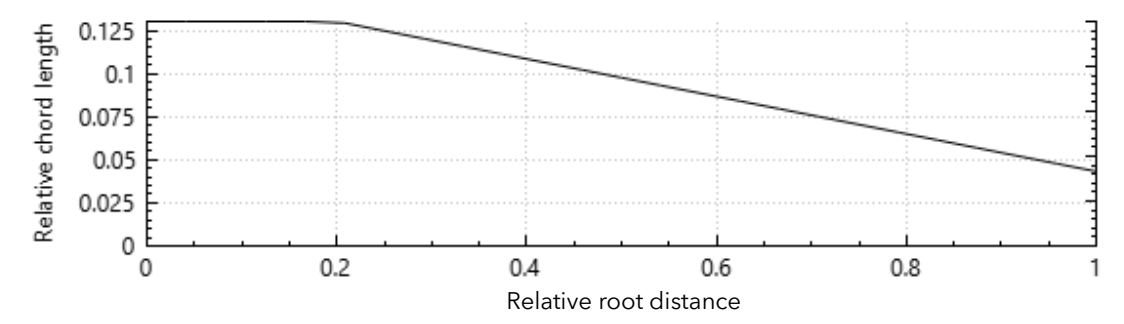


Figure 8 Optimised chord length distribution.

Figure 8 shows the optimised chord length distribution. Convergence tolerance limits were set at: objective function step of 0.01 and design variable step of 0.01. However, in this case the objective function was changing by $<10^{-4}$ when the variable tolerance was met, so this is definitely a good starting point to optimise from.

This required 23 function evaluations and took 20 minutes. The convergence tolerance could be set lower, but this would take much longer, and this analysis already gives a reasonable near-optimal distribution.

2.2 Twist Angle

The relative incoming wind velocity changes at each aerodynamical station with increasing radial distance. The root of the blade has a much lower rotational velocity than the tip, causing differing relative wind directions shown in Figure 9. This shows a root section (left) and tip section (right). Incoming wind speed (blue) represents a larger portion of the root relative wind direction (green) than the tip, where the rotational velocity (red) dominates the incoming wind direction. β (twist angle) should therefore be higher at the root so that the angle of attack is not so high that separation occurs (i.e.: to keep the airfoil operating efficiently).

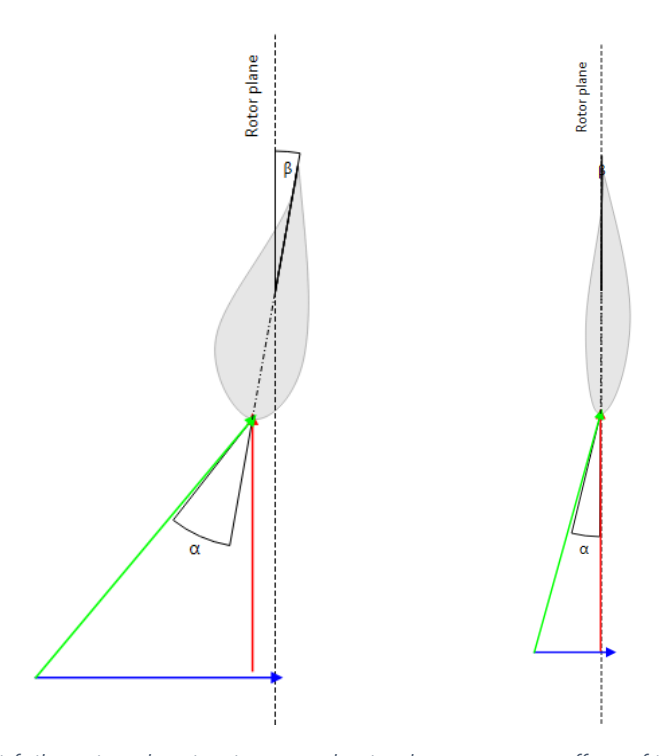


Figure 9 Left: root airfoil section showing increased twist due to greater effect of incoming wind, compared to tip airfoil section (right) with almost not twist due to high rotational velocity.

Twist angle was parameterised similarly to chord length by linearly varying twist along the blade. This is a good approach because it deals with the expected high twist at the root and low twist at the tip.

TwistDist.m uses 2 variables to define the root twist and the tip twist respectively, with other twists define on a linear progression.

Initially, to reduce computing time, the chord distribution was fixed at the optimum value found in the above analysis, and the twist varied to reach a point hopefully close to the optimum in a shorter time than running a 4-dimensional optimisation.

Nelder-Mead algorithm was initially used, but it failed to converge on a realistic optimum (0.02° root, 3.93° tip), which does not make physical sense as the root should be more twisted than the tip.

A global search (genetic algorithm) was applied to avoid getting stuck in local minima or 'flat' parts of the design space. Figure 10 shows this process part-way through. The number of function evaluations required made this prohibitively slow, but a good improvement to c_p =**44%** was achieved and constrained the design space enough that a local search algorithm could more confidently be implemented.

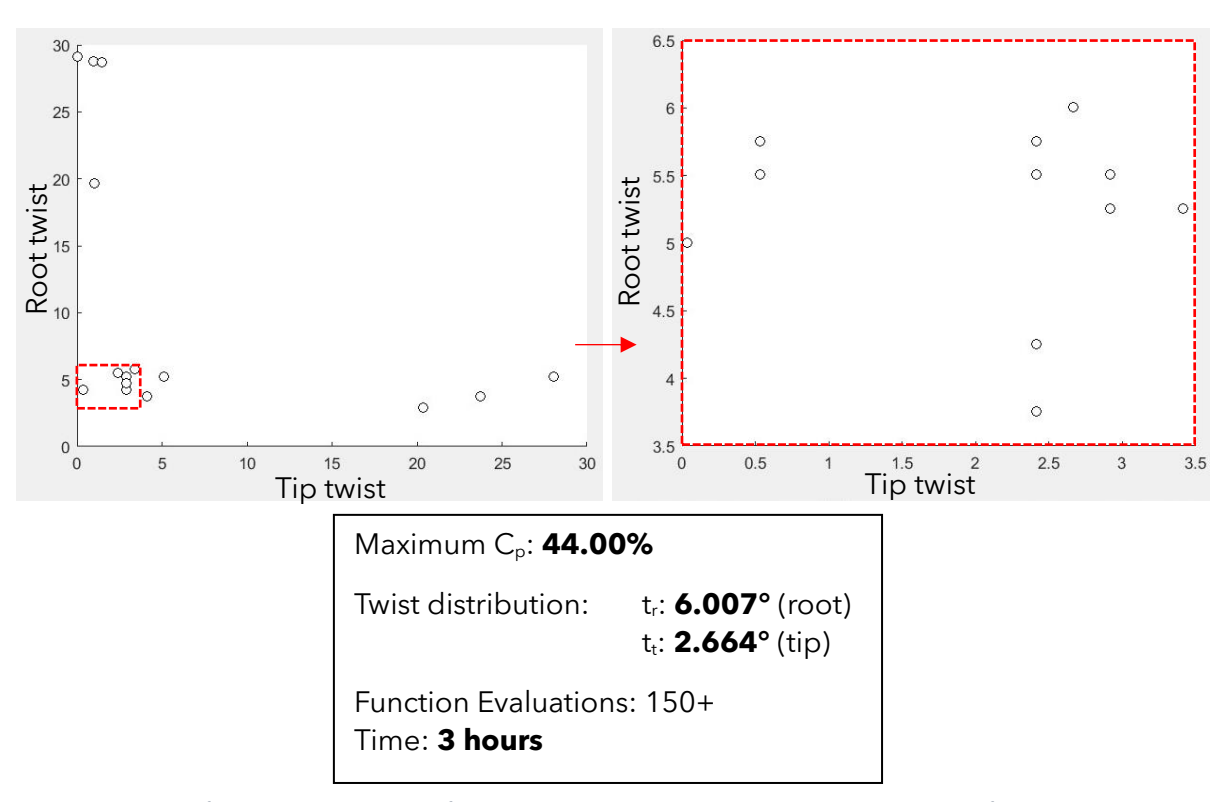


Figure 10 Left: Genetic algorithm after 3 iterations on twist angle, Right: Zoomed in, after 6 iterations.

This value is assumed to be close to the global optimum so is a useful starting point for the Nelder-Mead algorithm which is less likely to get stuck from a good starting point. Figure 11 shows the results of a Nelder-Mead optimisation starting from [6, 2](root, tip).

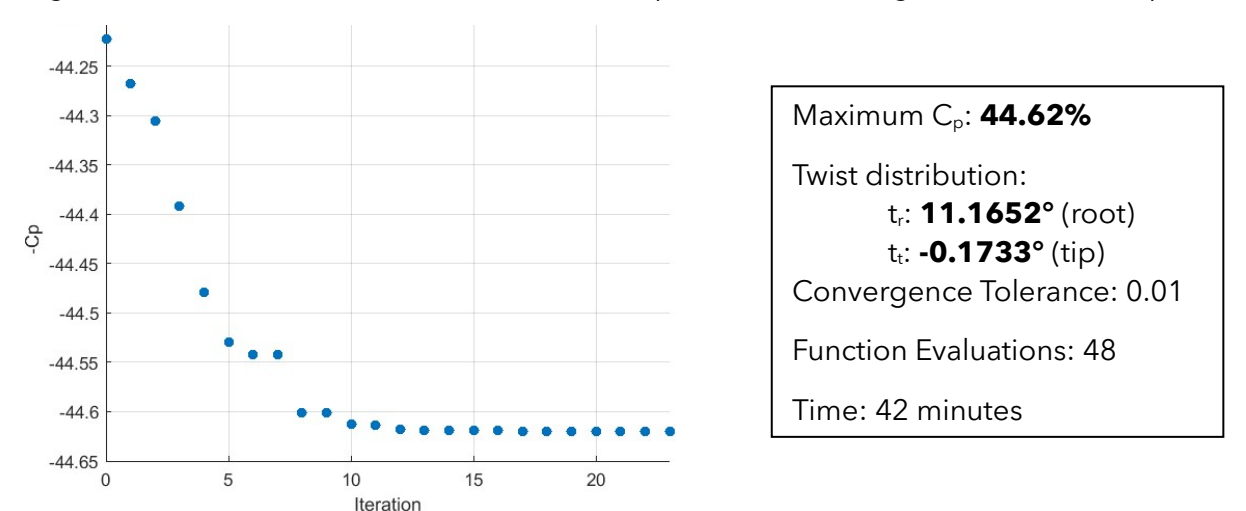


Figure 11 Convergence plot for twist angle distribution optimisation

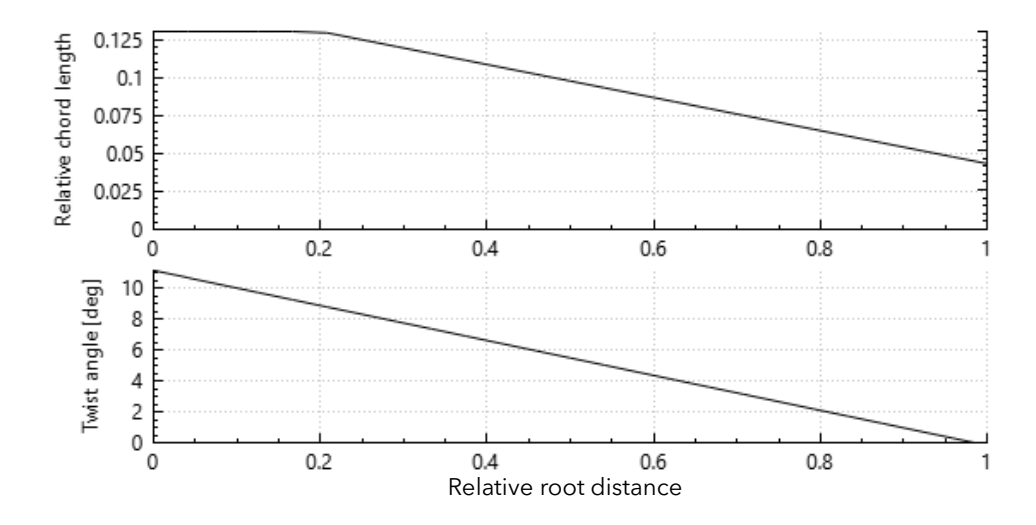


Figure 12 Optimised Chord and Twist angle distributions for a 1.1m blade.

At this point chord and twist distribution could be combined into a 4-dimensional optimisation. However, the result achieved here is likely close to optimal and was achieved in relatively short time. The framework set out here could handle many more design variables, but the short timescale of this project meant this approach was more suitable to demonstrate the methods and theory behind the optimisations, while also achieving a near-optimal result.

2.3 Airfoil Section

Selig (1998) proposes a set of low Reynolds number airfoils for small HAWT[9]. Table 1 shows these airfoils. SG6040 has the lowest design Reynolds number and is primarily designed for the root of the blade if large bending moments are expected. SG6041,42 and 43 are the primary airfoils that make up most of the blade.

Previous analysis uses SG6040 throughout as a reference.

Table 1 The airfoils used in this study, from Selig(1998)[9]

Airfoil	Design Re	Thickness	Blade Location
	200,000	16%	Root
SG 6043	250,000	10%	Mid-span
SG 6042	333,000	10%	Tip

To parameterise the airfoil distribution a step-function in conjunction with the floor function was used. Figure 13 shows the underlying function which steps from 1 to 3 over the blade length. Taking the floor of this function gives an integer from 1-3 at each aerodynamical station (Figure 14). The airfoil number equation is:

$$A_N = floor\left(\frac{2}{1 + e^{-j\left(x - \frac{i}{100}\right)}} + 1.1\right) : 0 < x < 1.1$$

- *i*: horizontal position of the step
- **j**: stretch in x-axis (radial distance) of the step (i.e.: blending zone size)

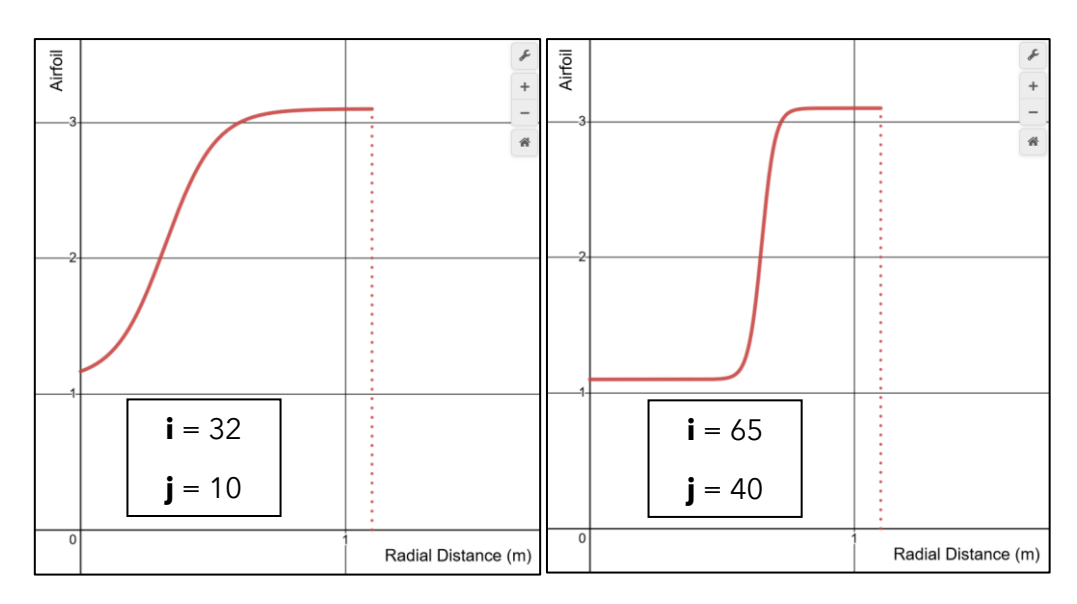


Figure 13 Airfoil distribution underlying function

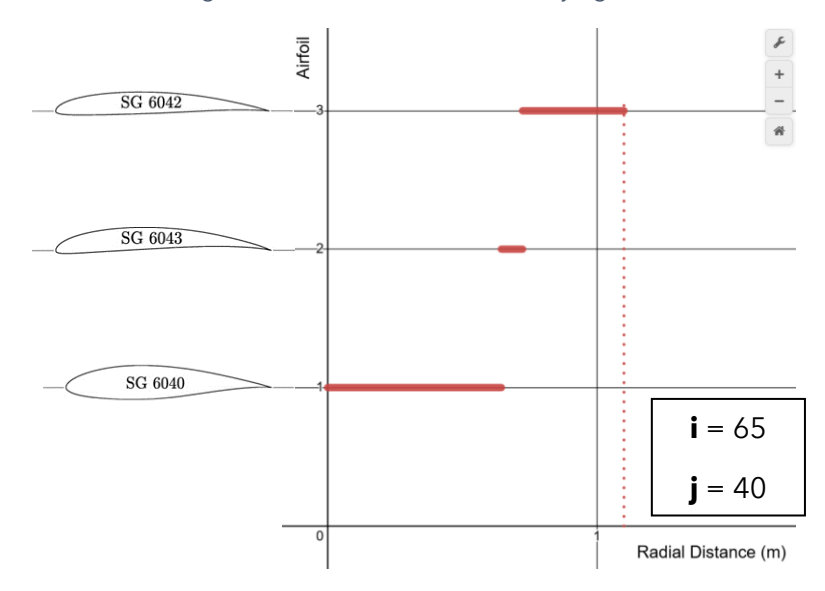


Figure 14 Airfoil distribution function with floor function applied to give discrete airfoil 'zones'.

The limitation here is that the airfoils cannot change order. The order is SG6040, SG6043, then SG6042 at the tip. If the blade starts with SG6043 there cannot be any SG6040 in this parameterisation. This is justified because the designed Reynolds number of each airfoil is increasing with distance along the blade, which lines up with expected behaviour - the root experiences lower rotational velocity so will require an airfoil designed for lower operating Reynolds numbers.

Figure 15 shows the results of 5 iterations of a genetic algorithm on the 2-variable design space to find a good estimation of the global optimum. For efficiency, the optimum chord and twist distributions are kept so this is still a 2-dimensional optimisation.

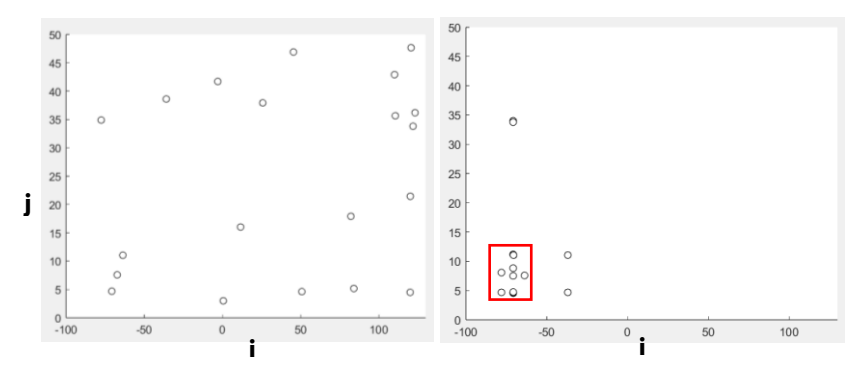


Figure 15 Genetic algorithm convergence for airfoil distribution

After 5 iterations:

•
$$\mathbf{i} = -70.7$$
; $\mathbf{j} = 4.5$, with $C_p = 44.75$ %

However, this highlights a problem with the airfoil distribution function. Figure 16 shows sections where the airfoil distribution is fully airfoil-3 or fully airfoil-1, rather than a mix. The optimiser struggled with these plateaus but ultimately began to converge on a purely airfoil 3 (SG6042) design.

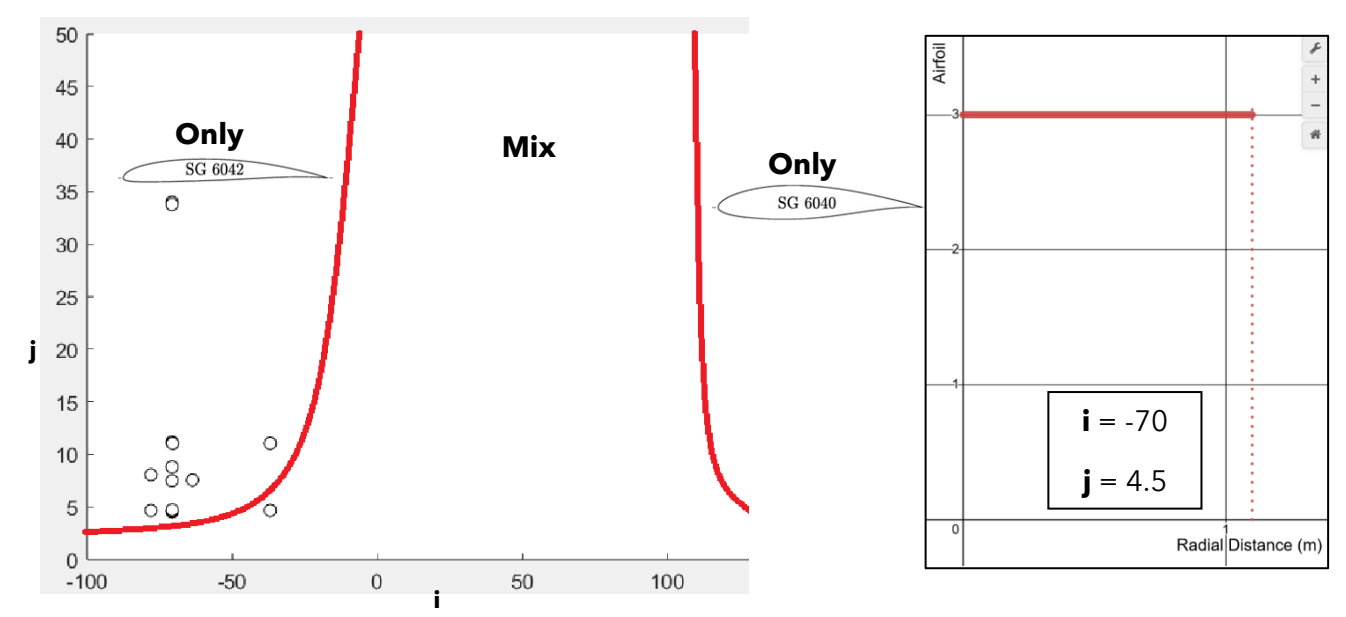


Figure 16 Left: design space highlighting objective function plateaus where airfoil distribution becomes constant. Right: visualisation of 'optimum' found by genetic algorithm (only airfoil 3)

To test if a blend of the chosen airfoils is really optimal, a blending region was set (i.e.: **j** was fixed). This created a 1D optimisation based on where the blending region occurs. Figure 17 shows the convergence plot (**j**=8).

The optimal result shifts the blending region outside of the blade so that only the first aerodynamical station is airfoil-2 - the rest are airfoil-3. This results in a Cp_{max} of **44.75%**.

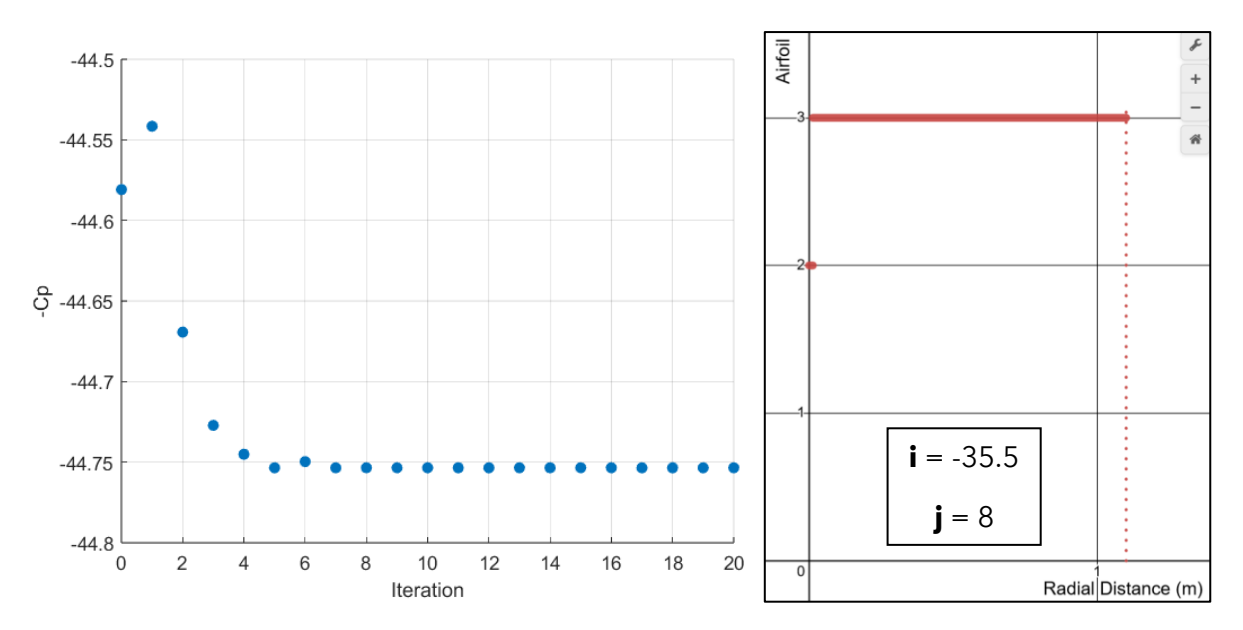


Figure 17 Left: convergence plot for varying position of airfoil blend region. Right: visualisation of the optimal airfoil distribution (only the first station is SG6043, the rest are SG6042)

3 Results

The final blade design is shown in Figure 18. Since each chord, twist and airfoil were varied separately before being combined this is likely not the global optimum. This approach is recommended in Stylianidis (2010)[7] as way to cut computation time but still reach a near-optimal solution.

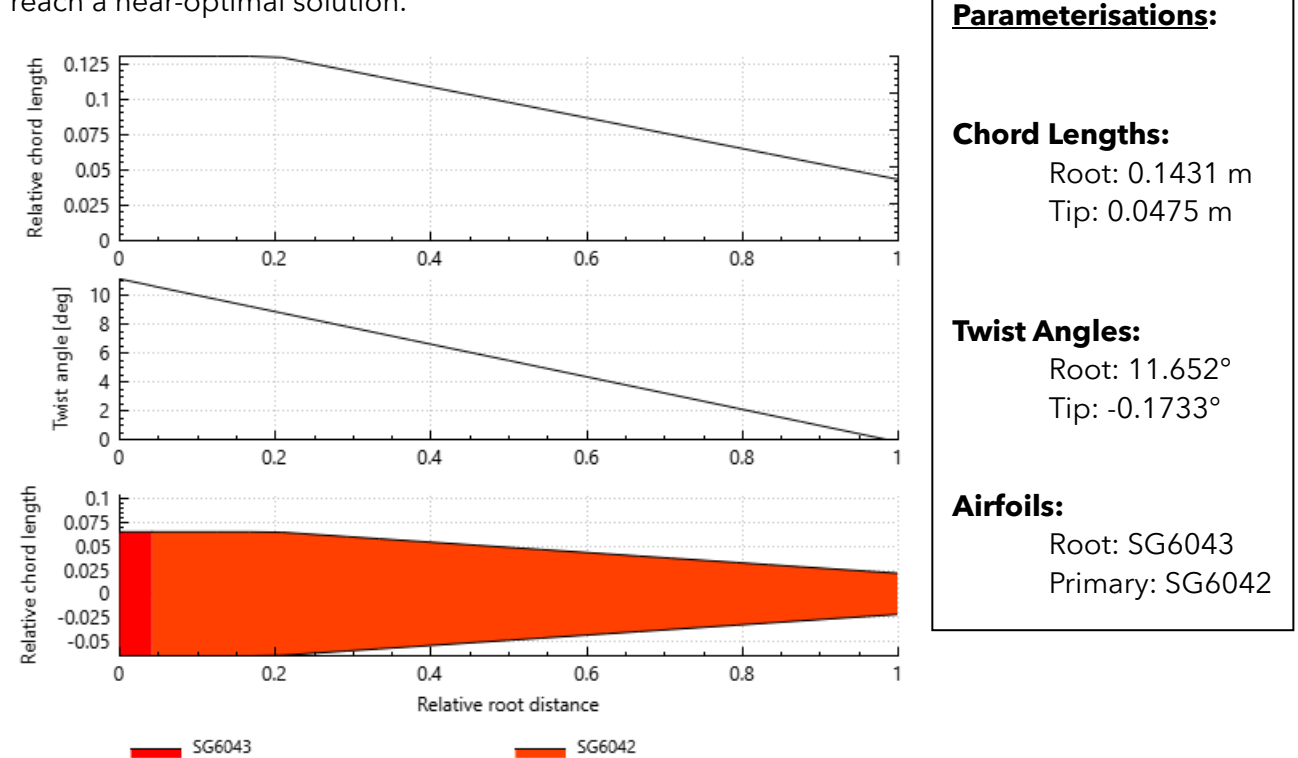


Figure 18 Optimised chord, twist, and airfoil distributions for a 1.1m blade

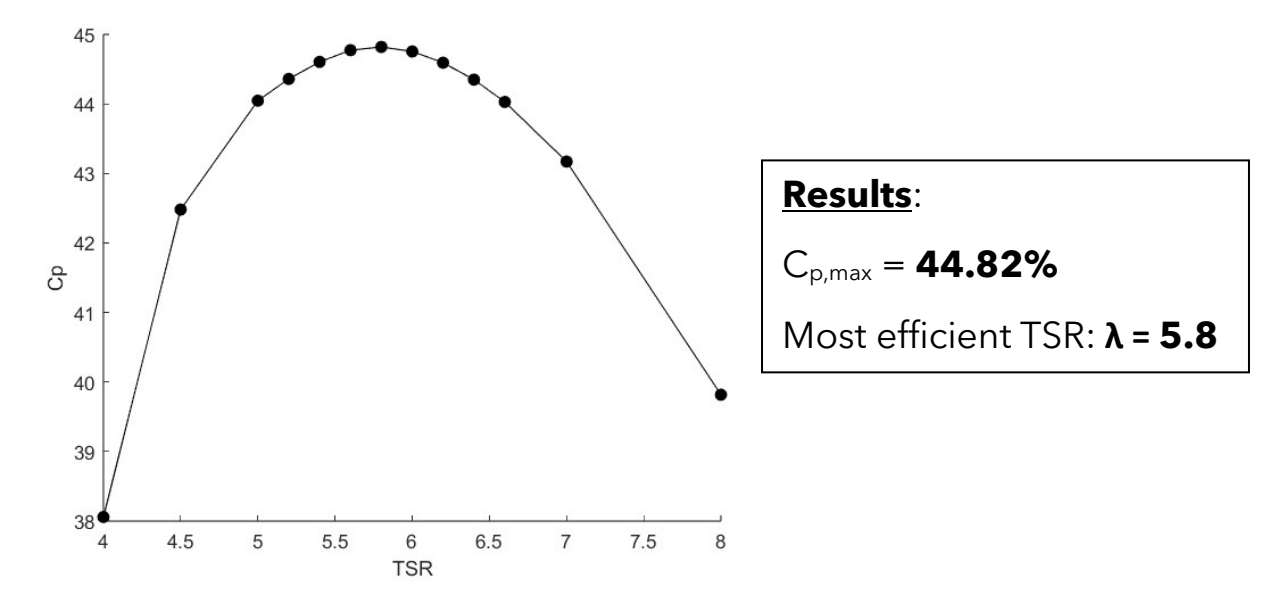


Figure 19 Final blade detailed TSR vs Cp curve to show maximum Cp=44.82% @ TSR=5.8

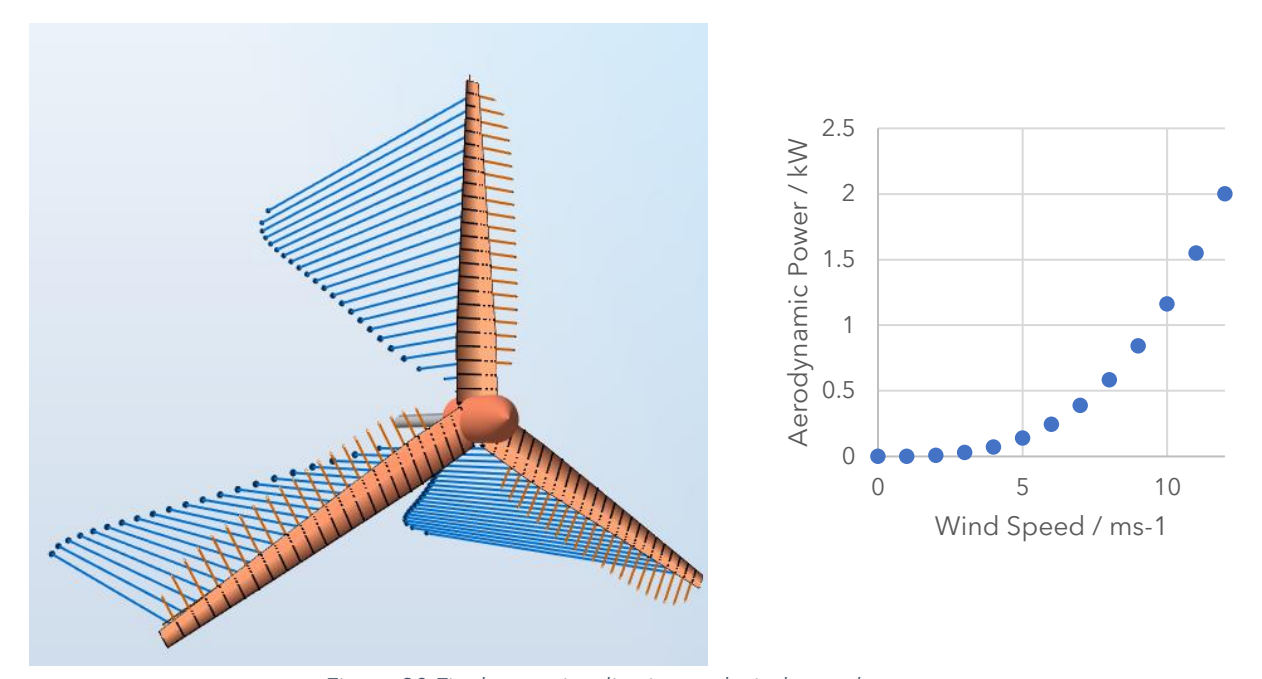


Figure 20 Final rotor visualisation and wind speed vs power curve

Figure 19 and Figure 20 show the performance characteristics of the final blade and rotor. A maximum C_p =**44.82%** was achieved at a TSR of 5.8. The wind speed vs. power curve shows power rapidly increasing - in reality there will be a maximum speed the turbine can safely rotate, limited by the gearbox and generator, to set a maximum power output.

Additionally, aerodynamic noise should be considered. This varies with the sixth power of windspeed, and a general rule-of-thumb is that tip speed should not exceed 60m/s[10]. At the optimum TSR (λ =5.8) this occurs at a wind speed of 10m/s. So above this the rotor speed should be limited. This is especially important for these small wind turbines which will be on residential property or attached to buildings, so they do not interfere with peoples' lives.

3.1 Optimisation discussion

The optimal chord distribution makes physical sense (narrowing towards the tip), as the tip section is experiencing much faster relative wind velocities. Thinner blades have lower drag, so to maximise the lift-drag ratio the blade must taper. Whereas the slower velocity and lower Reynolds number experienced at the root is better suited for larger chords which are more efficient at low Reynolds numbers.

The optimal twist angle aligns with expectations also since the increasing relative wind velocity and changing angle of attack along the blade mean that the blade should be more twisted at the root, getting closer to 0° twist at the tip. This ensures that the airfoils are not stalling from high angles of attack at the root, and also tunes the position of the tip airfoils to maximise lift-drag ratio. The final tip twist was just below 0°, this is likely not optimal but reflects the low fidelity linear parameterisation used. It likely constitutes a trade-off by optimising average lift-drag ratio across the blade – resulting in a slightly suboptimal twist at the tip. Defining twist distribution with a more complex parameterisation may yield better results that align with physical expectations.

The airfoil distribution optimisation was slightly more unexpected. Initially, the SG small HAWT airfoil family was used, however the optimiser favoured just the SG6042 airfoiltrying to eliminate the SG6040 and SG6043 sections.

This could be due to the omission of structural considerations. The thicker SG6040 is intended as a root airfoil to cope with increased bending moments, however this comes with an aerodynamic handicap. So it could be expected that SG6040 would be favoured if structural considerations were included, but since they are not the optimiser tries to removes the airfoil, in favour of the thinner airfoils with higher lift-drag ratios[9].

The graphs of the parameterisations can be found at https://www.desmos.com/calculator/9uf30talan

4 Reflection

Due to time available for this study, it was restricted in breadth to focus on just chord, twist, and airfoil distribution. In reality, there are many more important factors which affect the shape of the blade, and optimisation improvements which were not possible to implement in the short timescale.

4.1 Improved Parameterisation

The first optimisation improvement could be improving the way chord, twist and airfoil are parameterised.

Currently, the optimum twist distribution goes beyond 0° at the tip which does not reflect the expected physical behaviour. The angle of attack graph for the blade is shown in Figure 21. Due to the simple linearisation of twist angle, the middle section has a minimal angle of attack, while the root is very high - leading to degraded aerodynamic performance.

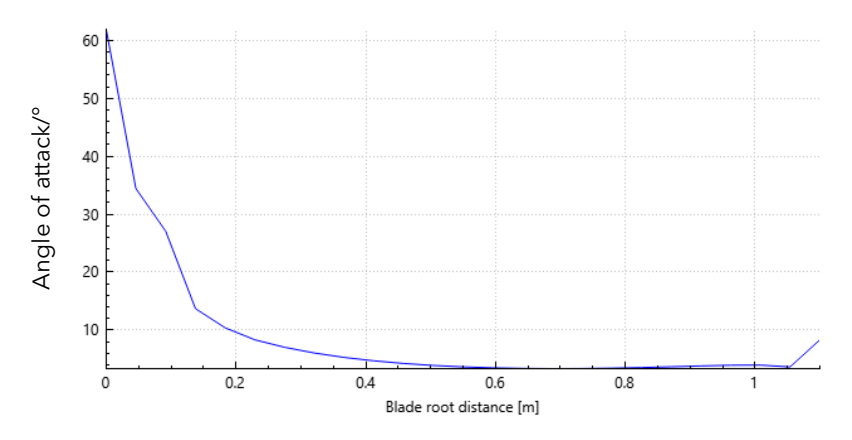


Figure 21 Current blade angle of attack distribution

An improvement could be to define the twist with a more complex function, using 3 or more variables. Figure 22 shows a quadratic distribution with variables to define the root and tip twist and how steepness of the curve in between. Another option would be using the velocity triangles in Figure 9, to show that relative wind direction varies with cos⁻¹x. Shown in Figure 22, this scheme uses 2 variables to change how steep the curve and how quickly it decreases. Since this matches the distribution of angle of attack this may be better suited to finding optimal lift-drag ratios of airfoils along the blade.

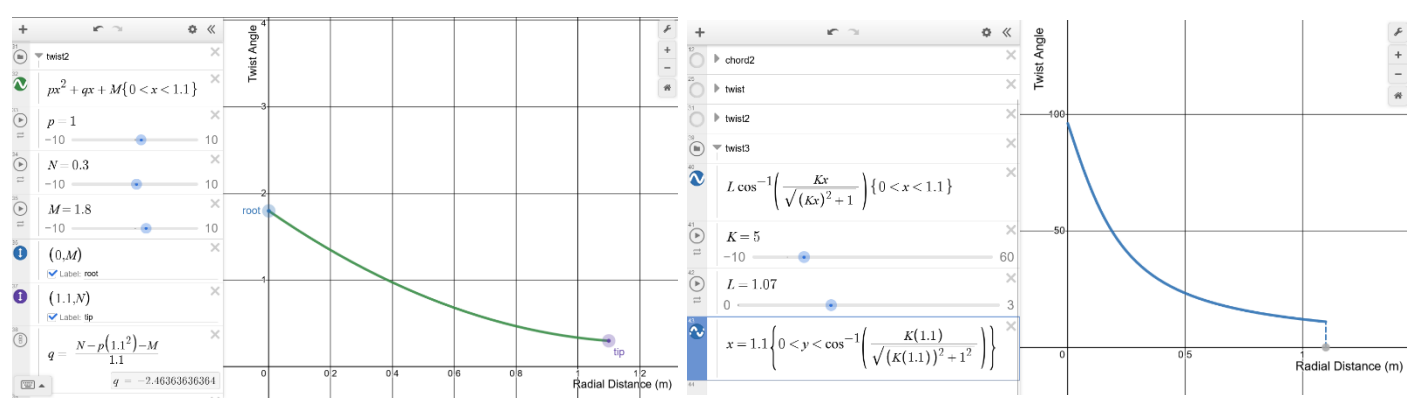


Figure 22 Alternative Twist distribution schemes for improved parameterisation. Quadratic distribution left, trigonometric right.

Similar parameterisation improvements could be applied to chord and airfoil distribution to allow them to get closer to the true optimal distributions.

4.2 Objective Function

Currently, the objective function simply finds the maximum C_p from a range of TSRs and optimises on this. As discussed in Section 2.1, this disregards structural and cost concerns. Ashes is capable of simulating the structural loads in the blade so this would simply involve modifying the objective function to extract this data.

The structural data could be used with known yield strengths of blade materials to apply a penalty function to any thin blade geometries that generate excessive bending moments.

Cost could be approximated in the objective function using total volume of the blade, which is a good proxy of cost without knowledge of the manufacturing processes or material cost. This could be combined with C_p to generate a rough cost per unit power metric.

Both of these modifications would transform the objective function from maximum C_p to a cost of power optimisation with structural constraints to prevent excessive bending moments.

4.3 Manufacturing Considerations

More complex parameterisations may yield a more efficient blade but there are also benefits to further <u>simplifying</u> the blade. Figure 23 shows the efficiency loss incurred by using simpler chord distributions. The losses from simplification of the blade can be justified by significant savings during production[8]. This becomes increasingly important when the number of units produced increases - making blade simplification more desirable for small wind turbines so they can be sold more cheaply in higher numbers.

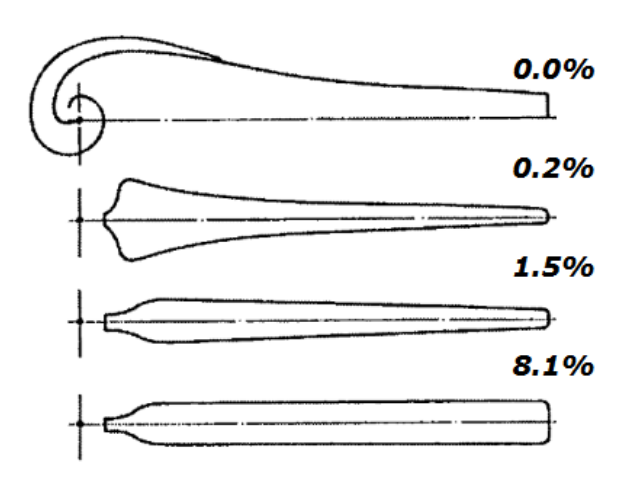


Figure 23 Efficiency losses from simplification compared to ideal chord length blade.

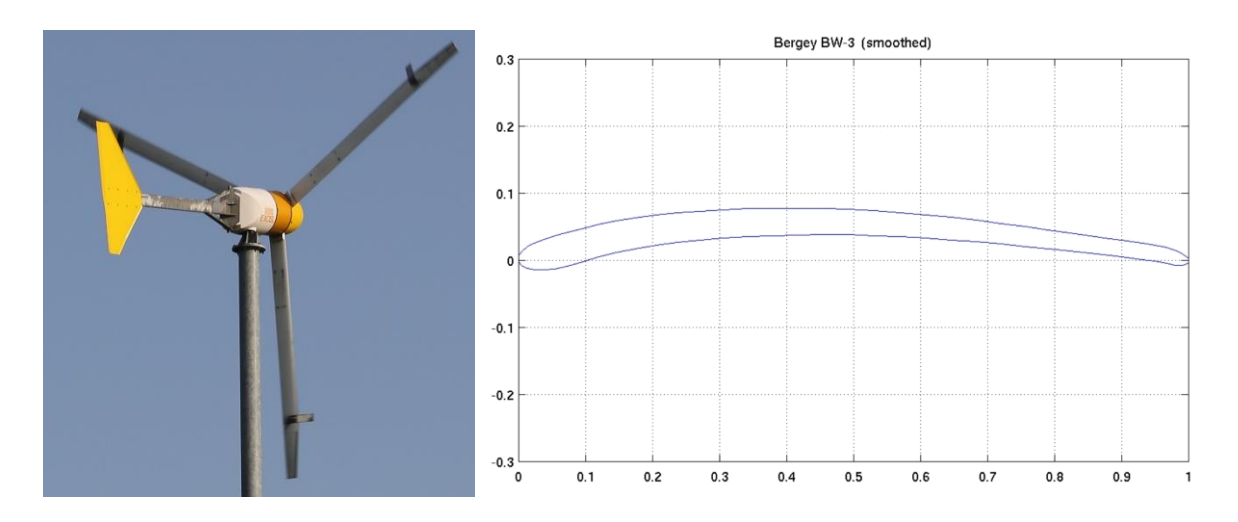


Figure 24 Left: Bergey Windpower small HAWT[11]. Right: BW-3 airfoil

This trade-off can be seen in Bergey wind turbines (Figure 24) - commercial small HAWT. These use an almost constant chord length with minimal twist, evidently evaluating that savings in blade production offset any losses in efficiency.

Figure 24 also highlights another aspect of manufacturing considerations that are difficult to incorporate into an optimisation. The BW-3 airfoil used by Bergey is optimised for pultrusion (it can be manufactured easily). The SG-family of low Reynolds number airfoils may be slightly more optimal, but ultimately the small increase in power may be offset by significantly higher production costs.

Overall, it would be best to take a holistic approach - incorporating more sophisticated optimisation techniques and a more detailed objective function, but also keeping in mind manufacturing considerations such as quantity, cost and ease of manufacture when making design decisions.

References

- [1] R. Wiser and M. Bolinger, 'Land-Based Wind Market Report: 2023 Edition', US Department of Energy, 2023.
- [2] 'The Town and Country Planning (General Permitted Development) (England) Order 2015'. Accessed: Jan. 07, 2024. [Online]. Available: https://www.legislation.gov.uk/uksi/2015/596/made
- [3] 'Class H Wind turbines on residential property'. Accessed: Jan. 07, 2024. [Online]. Available: https://www.planninggeek.co.uk/gpdo/renewable-energy/class-h/
- [4] 'Betz limit Energy Education'. Accessed: Jan. 07, 2024. [Online]. Available: https://energyeducation.ca/encyclopedia/Betz_limit
- [5] CFD-based wind turbine aerodynamic shape optimization, (Apr. 24, 2019). Accessed: Jan. 07, 2024. [Online Video]. Available: https://www.youtube.com/watch?v=5qSY7lbUuMA
- [6] D. Darling, 'tip speed ratio'. Accessed: Jan. 07, 2024. [Online]. Available: http://www.daviddarling.info/encyclopedia/T/AE_tip_speed_ratio.html
- [7] N. Stylianidis, T. Macquart, and A. Maheri, 'Aerodynamic design of wind turbine blades considering manufacturing constraints', in 3rd International Symposium on Environmental Friendly Energies and Applications (EFEA), Saint Ouen, Paris, France: IEEE, Nov. 2014, pp. 1-6. doi: 10.1109/EFEA.2014.7059984.
- [8] P. J. Schubel and R. J. Crossley, 'Wind Turbine Blade Design', *Energies*, vol. 5, no. 9, Art. no. 9, Sep. 2012, doi: 10.3390/en5093425.
- [9] P. Gigue`re and M. S. Selig, 'New Airfoils for Small Horizontal Axis Wind Turbines', Journal of Solar Energy Engineering, vol. 120, no. 2, pp. 108–114, May 1998, doi: 10.1115/1.2888052.
- [10] G. Leloudas, W. J. Zhu, J. N. Sørensen, W. Z. Shen, and S. Hjort, 'Prediction and Reduction of Noise from a 2.3 MW Wind Turbine', J. Phys.: Conf. Ser., vol. 75, no. 1, p. 012083, Jul. 2007, doi: 10.1088/1742-6596/75/1/012083.
- [11] L. Bauer, 'Bergey BWC Excel 10 10,00 kW Wind turbine'. Accessed: Jan. 11, 2024. [Online]. Available: https://en.wind-turbine-models.com/turbines/501-bergey-bwc-excel-10